

Article type : Original

## Mast Cells Promote Non-Alcoholic Fatty Liver Disease Phenotypes and Microvesicular Steatosis in Mice Fed Western Diet

Lindsey Kennedy<sup>2</sup>, Vik Meadows<sup>2</sup>, Amelia Sybenga<sup>6</sup>, Jennifer Demieville<sup>4</sup>, Lixian Chen<sup>2</sup>, Laura Hargrove<sup>5</sup>, Burcin Ekser<sup>3</sup>, Wasim Dar<sup>7</sup>, Ludovica Ceci<sup>2</sup>, Debjyoti Kundu<sup>2</sup>, Konstantina Kyritsi<sup>2</sup>, Linh Pham<sup>2&</sup>, Tianhao Zhou<sup>5</sup>, Shannon Glaser<sup>5</sup>, Fanyin Meng<sup>1,2</sup>, Gianfranco Alpini<sup>1,2</sup> and Heather Francis<sup>1,2</sup>

<sup>1</sup>Richard L. Roudebush VA Medical Center, <sup>2</sup>Division of Gastroenterology and Hepatology, Department of Medicine, <sup>3</sup>Department of Transplant Surgery, Indiana University School of Medicine, Indianapolis, IN; <sup>4</sup>Central Texas Veterans Health Care System and <sup>5</sup>Department of Medical Physiology, Texas A&M University College of Medicine, Bryan, TX; <sup>6</sup>Department of Pathology, Microbiology, and Immunology, Vanderbilt University School of Medicine, Nashville, TN; <sup>7</sup>Division of Immunology and Organ Transplantation, Department of Surgery, University of Texas Health Science Center at Houston, Houston, TX.

<sup>&</sup>current address: Texas A&M University-Central Texas, Department of Science & Mathematics, Killeen, Texas.

**Keywords:** mast cells; microvesicular steatosis; non-alcoholic steatohepatitis; fibrosis; inflammation; aldehyde dehydrogenase 1 family, member A3, miR-144-3p

### Address correspondence to:

Heather Francis, Ph.D., FAASLD

This article has been accepted for publication and undergone full peer review but has not been through the copyediting, typesetting, pagination and proofreading process, which may lead to differences between this version and the [Version of Record](#). Please cite this article as [doi: 10.1002/HEP.31713](#)

This article is protected by copyright. All rights reserved

Professor of Medicine and VA Research Career Scientist  
Indiana University, Gastroenterology, Medicine  
Richard L. Roudebush VA Medical Center  
702 Rotary Circle, Rm. 013C  
Indianapolis, IN 46202-2859  
heafrcn@iu.edu  
317-278-4222

### **Abbreviations:**

Acaca = acetyl-CoA carboxylase 1; ALDH1A3 = aldehyde dehydrogenase 1 family, member A3; ALT = alanine aminotransferase; AST = aspartate aminotransferase; BDL = bile duct ligation; BS = basal; BW = body weight; CCA = cholangiocarcinoma; CCL = C-C motif ligand; CD = control diet; CK-19 = cytokeratin-19; c-Kit = KIT proto-oncogene receptor tyrosine kinase; Col1a1 = collagen type1  $\alpha$ 1; Cpt = carnitine palmitoyltransferase; EIA = enzyme immunoassay; FASN = fatty acid synthase; FFA = free fatty acids; H&E = hematoxylin and eosin; HFD=high fat diet; HSC = hepatic stellate cell; hH = human hepatocytes; IFN- $\gamma$  = interferon- $\gamma$ ; IgE = immunoglobulin E; IGF-1 = insulin-like growth factor-1; IL = interleukin; IPA = ingenuity pathway analysis; KC = Kupffer cell; *Kit*<sup>W-sh</sup> = B6.Cg-*Kit*<sup>W-sh</sup>/HNihrJaeBsmJ; LW = liver weight; MC = mast cell; MDA = malondialdehyde; miR-144-3p = microRNA 144-3 prime; mMCP-1 = mouse MC protease-1; NAFLD = non-alcoholic fatty liver disease; NASH = non-alcoholic steatohepatitis; OA = oleic acid; p16 = cyclin-dependent kinase inhibitor 2A; p18 = cyclin-dependent kinase inhibitor 2C; p21 = cyclin-dependent kinase inhibitor 1A; PA = palmitic acid; PAI-1 = serpine-1; PBS = phosphate buffered saline; PPAR- $\alpha$  = peroxisome proliferator-activated receptor- $\alpha$ ; PPAR- $\gamma$  = peroxisome proliferator-activated receptor- $\gamma$ ; PSC = primary sclerosing cholangitis; qPCR = quantitative polymerase chain reaction; SA = stearic acid; SA- $\beta$ -Gal = senescence-associated- $\beta$ -galactosidase; TG = triglycerides; VEGF-A = vascular endothelial growth factor-A; vWF = vonWillebrand factor; WD = Western diet; WT = wild-type

### **Financial Support:**

This work was supported by the Hickam Endowed Chair, Gastroenterology, Medicine, Indiana University and the Indiana University Health – Indiana University School of Medicine Strategic Research Initiative, the SRCS Award and VA Merit awards to Dr. Alpini (5I01BX000574) and Dr. Francis (1I01BX003031) from the United States Department of Veteran's Affairs, Biomedical

Laboratory Research and Development Service and NIH grants DK108959 and DK119421 to Dr. Francis and DK054811 to Drs. Alpini and Glaser. This material is the result of work supported by resources at the Central Texas Veterans Health Care System, Temple, TX and Richard L. Roudebush VA Medical Center, Indianapolis, IN. The views expressed in this article are those of the authors and do not necessarily represent the views of the Department of Veterans Affairs.

**Conflict of interest:** The authors have no conflicts of interest to disclose.

**Author contributions:**

LK: conceptualization, data curation, formal analysis, investigation, methodology, validation, visualization, writing – original draft, writing – review & editing; VM: data curation, formal analysis, investigation, methodology, validation and writing – review & editing; AS: formal analysis, investigation, validation and writing – review & editing; LC: data curation, formal analysis, writing – editing; DK: data curation, formal analysis, investigation, methodology, validation and writing – review & editing; JD: data curation, formal analysis, investigation, methodology and validation; LH: data curation, formal analysis, investigation, methodology and validation; BE: resources; WD: resources and data curation; LC: data curation, formal analysis, investigation, methodology and validation; KK: data curation, formal analysis, investigation, methodology and validation; LP: data curation, formal analysis, investigation, methodology and validation; TZ: software; SG: funding acquisition, resources; FM: writing – review & editing; GA: funding acquisition, resources, writing – review & editing; HF: conceptualization, formal analysis, funding acquisition, project administration, resources, supervision, visualization, writing – review & editing

## Abstract

**Background & Aims:** Non-alcoholic fatty liver disease (NAFLD) is simple steatosis, but can develop into non-alcoholic steatohepatitis (NASH) characterized by liver inflammation, fibrosis and microvesicular steatosis. Mast cells (MCs) infiltrate the liver during cholestasis and promote ductular reaction (DR), biliary senescence and liver fibrosis. We aimed to determine the effects of MC depletion during NAFLD/NASH. **Approach & Results:** Wild-type (WT) and *Kit<sup>W-sh</sup>* (MC-deficient) mice were fed control (CD) or a Western diet (WD) for 16 wks; select WT and *Kit<sup>W-sh</sup>* WD mice received tail vein injections of MCs 2X/wk for 2 wks prior to sacrifice. Human samples were collected from normal, NAFLD or NASH. Cholangiocytes from WT WD mice and human NASH have increased insulin-like growth factor (IGF)-1 expression that promotes MC migration/activation. Enhanced MC presence was noted in WT WD mice and human NASH, along with increased DR. WT WD mice had significantly increased steatosis, DR/biliary senescence, inflammation, liver fibrosis and angiogenesis compared to WT CD mice, which was significantly reduced in *Kit<sup>W-sh</sup>* WD mice. Loss of MCs prominently reduced microvesicular steatosis in zone 1 hepatocytes. MC injection promoted WD-induced biliary and liver damage, and specifically upregulated microvesicular steatosis in zone 1 hepatocytes. Aldehyde dehydrogenase 1 family, member A3 (ALDH1A3) expression is reduced in WT WD mice and human NASH, but increased in *Kit<sup>W-sh</sup>* WD mice. miR-144-3p expression was increased in WT WD mice and human NASH, but reduced in *Kit<sup>W-sh</sup>* WD mice, and was found to target ALDH1A3. **Conclusions:** MCs promote WD-induced biliary and liver damage, and may promote microvesicular steatosis development during NAFLD progression to NASH via miR-144-3p/ALDH1A3 signaling. Inhibition of MC activation may be a therapeutic option for NAFLD/NASH treatment.

Non-alcoholic fatty liver disease (NAFLD) can develop into non-alcoholic steatohepatitis (NASH)(1). High mortality rates are seen in NAFLD patients, and NASH is the third most common indication for liver transplantation in the U.S.(2, 3). During NAFLD, macrovesicular steatosis is characterized as hepatocytes with a single, large vacuole of fat that displaces the nucleus and is considered benign(4). Microvesicular steatosis, in NASH, is described as hepatocytes with

numerous, small lipid vesicles that do not displace the nucleus, entailing a more severe prognosis(4, 5). Ductular reaction (DR) and biliary senescence are found in NASH patients, and DR positively correlates with liver fibrosis during NASH(6, 7).

Mast cells (MCs) are key mediators of allergies and inflammation(8). MC number increases in cholangiopathies, such as primary sclerosing cholangitis (PSC) and cholangiocarcinoma (CCA), and in the bile duct ligated (BDL) and multidrug resistance 2-knockout ( $Mdr2^{-/-}$ ) mouse models of cholestasis(9-11). We have demonstrated that (i) MCs reside near injured ducts, (ii) MC infiltration is preceded by cholangiocyte proliferation following BDL(10-12) and (iii) inhibition or genetic loss of MCs reduces DR, biliary senescence and liver fibrosis in BDL and  $Mdr2^{-/-}$  mice(9, 10). Serum histamine (released by activated MCs) levels increase in NAFLD and NASH patients(6); however, the direct role of MCs is unknown.

MicroRNAs (miRs) are dysregulated during NAFLD, and can be diagnostic or prognostic markers during disease progression(13). Hepatic miR-144-3p expression increases in NASH individuals(13); however, another group has found that miR-144-3p is reduced in Kupffer cells (KCs) from rats fed high fat diet (HFD)(13). The direct role of miR-144-3p during NAFLD/NASH is controversial.

Aldehyde dehydrogenase 1 family, member A3 (ALDH1A3) detoxifies aldehydes generated by lipid peroxidation(14). Lipid peroxidation occurs when oxidants attack lipids containing carbon-carbon double bonds leading to production of malondialdehyde (MDA)(15). Hepatic ALDH1A3 expression is reduced in human NAFLD and NASH(16), and enhanced lipid peroxidation correlates with hepatic steatosis and liver fibrosis in NASH(17). Additionally, lipid peroxidation increases microvesicular steatosis, which is accompanied by reduced  $\beta$ -oxidation(18, 19).

We evaluated the role of MCs in the progression of steatosis, DR, biliary senescence, inflammation, liver fibrosis and angiogenesis in a mouse model of NAFLD using a Western diet (WD, high-fat, trans-fat with high cholesterol and high fructose corn syrup equivalent) feeding model. Our data indicate a role for MCs in the induction of WD-induced phenotypes including microvesicular steatosis through miR-144-3p/ALDH1A3 signaling.

## Materials and Methods

### Materials

Total RNA was isolated from liver tissues, selected cell lines and isolated cholangiocytes and hepatocytes using TRI Reagent. miRNA was isolated from liver tissues and isolated hepatocytes

using the mirVana miRNA Isolation Kit (Ambion; Mountain View, CA). mRNA was reverse transcribed with the iScript cDNA synthesis kit (Bio-Rad; Hercules, CA). Primers were purchased from Qiagen (Valencia, CA) and described in Supplemental Table 1. qPCR was performed using RT<sup>2</sup> SYBR Green/ROX quantitative PCR master mix for the Applied Biosystems ViiA7 qPCR system (Life Technologies; Carlsbad, CA). For mouse and human staining, formalin-fixed paraffin-embedded samples were sectioned at 4-6  $\mu$ m; OCT-embedded sections were sectioned at 6-8  $\mu$ m; at least 10 fields were analyzed. Antibodies are described in Supplemental Table 2. All other reagents, chemicals and cell culture details are provided in Supplemental Data.

### **Animal Models**

Animal procedures were performed according to protocols approved by Baylor Scott & White Health and Indiana University School of Medicine (IUSM) IACUC committees. MC-deficient mice (B6.Cg-*Kit*<sup>W-sh</sup>/HNihrJaeBsmJ, i.e., *Kit*<sup>W-sh</sup>) and background-matched wild-type (C57BL/6J, i.e., WT) were purchased from Jackson Laboratory (Bar Harbor, ME). Animals were housed in microisolator cages in a temperature-controlled environment with 12:12 hour light-dark cycles. Studies were performed in 4 wk old male WT and *Kit*<sup>W-sh</sup> mice fed control diet (CD) consisting of standard chow and reverse osmosis water, or WD consisting of high-fat trans-fat diet (45% calories from fat and 0.2% cholesterol; Envigo; Indianapolis, IN) coupled with 55% fructose, 45% glucose w/w dissolved in reverse osmosis water for 16 wks, which induces steatosis, inflammation and fibrosis in normal mice(6). Selected WT WD and *Kit*<sup>W-sh</sup> WD mice received tail vein injections of 5x10<sup>6</sup> tagged (PKH26 Red Fluorescent Cell Linker), cultured MCs (MC/9, ATCC, CRL-8306) suspended in 0.1mL of 1X phosphate buffered saline (PBS), or 0.1mL 1X PBS 2X/wk for 2 wks following 14 wks of feeding. Animal numbers for each group are as follows: WT CD n=15 mice; WT WD n=10 mice; *Kit*<sup>W-sh</sup> CD n=8 mice; *Kit*<sup>W-sh</sup> WD n=13 mice; WT WD+MC n=13 mice; and *Kit*<sup>W-sh</sup> WD+MC n=11 mice. Liver tissues, serum, hepatocytes and cholangiocytes were collected(6, 9). Cholangiocytes were isolated using a monoclonal antibody (IgM, a gift from Dr. Ronald A. Faris, Brown University, Providence, RI)(10).

### **Human Samples**

Human liver tissues were collected from patients diagnosed with NAFLD or NASH, and non-diseased controls by Dr. Wasim Dar at UT Health School of Medicine and Dr. Burcin Ekser at IUSM, or were purchased from Sekisui XenoTech, LLC (Kansas City, KS); these samples were used for

RNA extraction, protein extraction and liver sections for staining. Explant tissues were obtained from transplant, and the diagnosis of NAFLD or NASH was determined by clinical, imaging and pathological analyses. Written informed consent was obtained from each patient and the study protocol conformed to the ethical guidelines of the 1975 Declaration of Helsinki as reflected in a priori approval by the UT Health Medical Center and IU IRB (no donor organs were obtained from executed prisoners or other institutionalized persons). Samples were deidentified, and patient information are provided in Supplemental Table 3. All other experimental procedures are detailed in Supplemental Data.

### **Statistical Analysis**

Data are expressed as the mean  $\pm$  SEM. Differences between groups were analyzed by the student unpaired *t* test when 2 groups were analyzed, and by two-way ANOVA when more than 2 groups were analyzed.

### **Results**

#### ***Biliary-Derived IGF-1 Drives MC Migration and MC Infiltration/Activation Increases During NAFLD/NASH***

We first evaluated changes in cytokine release from cholangiocytes isolated from WT CD and WT WD mice to determine potential MC chemoattractant candidates. We found that several interleukins and growth factors along with leptin and resistin increased in cholangiocyte supernatants from WT WD mice compared to WT CD mice (Figure 1A), and the fold-change of insulin-like growth factor-1 (IGF-1) secretion had the highest change (Figure 1B). Hepatic IgE levels, a key mediator of MC histamine release, increased in WT WD mice compared to WT CD mice (Figure 1C); however, IgE release from cholangiocytes was not detected (data not shown). To evaluate cholangiocyte-derived factors, we verified our multiELISA findings by increased IGF-1 secretion in cholangiocyte supernatants and serum (Figure 1D) and expression in liver sections (Figure 1E) in WT WD mice compared to WT CD mice. Notably, MCs have previously been shown to express and be activated by IGF-1(20). In human samples, we found an increase in IGF-1 immunoreactivity in NASH compared to controls (Figure 1F). Lastly, *in vitro*, we verified that inhibition of IGF-1 receptor (IGF-1R) blocks MC migration. We found that free fatty acid (FFA)-treated cholangiocyte supernatants induce MC migration, which is blocked following treatment with the IGF-1R inhibitors, AG 583, Linsitinib or PPP (Supplemental Figure 1).

In WT WD mice, MC (red arrows) numbers increased compared to WT CD mice, and were found primarily surrounding bile ducts (10-12) as shown by mMCP-1 staining (Figure 2A). Furthermore, hepatic expression of chymase, tryptase and c-Kit (MC-specific markers, Figure 2B) and serum histamine levels (Figure 2C) increased in WT WD mice compared to WT CD mice.

MC presence (tryptase, red) slightly increased in NAFLD, and increased in NASH compared to control samples; increased MC presence corresponded with enhanced DR (CK-19, brown), and MCs were found surrounding bile ducts (Figure 2D). These findings were supported by increased MC marker expression in NASH, with trend toward increasing in NAFLD, compared to control (Figure 2E).

### **MC Depletion Decreases WD-Induced Liver Damage and Steatosis**

We determined the role of MCs in WD-induced damage by feeding WT or *Kit<sup>W-sh</sup>* mice CD or WD for 16 wks (Supplemental Figure 2A). Macroscopic images showed that livers of WT WD mice were pale compared to WT CD mice; no significant color changes were noted in *Kit<sup>W-sh</sup>* CD or WD mice (Supplemental Figure 2B). Overall, WT WD mice had increased liver weight (LW) and LW/Body weight (BW) ratio compared to WT CD mice, which was reduced in *Kit<sup>W-sh</sup>* WD mice compared to WT CD mice; no changes were noted in BW between all groups (Supplemental Figure 2C). H&E staining showed that WT WD mice have >95% of hepatocyte involvement in macrovesicular and microvesicular steatosis in zone 1 and zone 2, with small lymphocytic aggregates, and WT WD mice were diagnosed with severe steatosis (Figure 3A). *Kit<sup>W-sh</sup>* WD mice presented with 50-70% hepatocytes involved in steatosis, with macrovesicular steatosis found in zone 1 and microvesicular steatosis found in zone 2, with no increase in inflammation, and were diagnosed with moderate steatosis (Figure 3A). Serum levels of alanine aminotransferase (ALT) increased in WT WD mice compared to WT CD mice, but reduced in *Kit<sup>W-sh</sup>* WD mice compared to WT WD mice (Figure 3B). Importantly, MC depletion decreased microvesicular steatosis in zone 1, which lies adjacent to the portal triad, that was present in WT WD mice.

Oil Red O staining and semi-quantification shows increased hepatic steatosis in WT WD mice compared to WT CD; however, *Kit<sup>W-sh</sup>* WD mice had reduced hepatic steatosis compared to WT WD mice (Figure 3C). Similarly, hepatic triglyceride (TG) levels increased in WT WD mice compared to WT CD mice, but reduced in *Kit<sup>W-sh</sup>* WD mice compared to WT WD mice (Figure 3C). Hepatocyte expression of lipogenesis markers increased in WT WD mice compared to WT CD mice, but were decreased in *Kit<sup>W-sh</sup>* WD mice compared to WT CD mice (Figure 3D). Conversely,  $\beta$ -oxidation

markers decreased in WT WD mice compared to WT CD mice, whereas *Kit<sup>W-sh</sup>* WD mice had increased expression of β-oxidation markers compared to WT WD mice (Figure 3D).

#### **WD-Induced DR and Biliary Senescence Decreased in MC-Deficient Mice**

We found increased DR (Figure 4A) and biliary proliferation (Figure 4B) in WT WD mice compared to WT CD mice, which were reduced in *Kit<sup>W-sh</sup>* WD mice compared to WT WD mice. Aside from DR, biliary senescence is enhanced in NAFLD and NASH patients(6), and we found increased biliary senescence in WT WD mice compared to WT CD mice shown by p16, SA-β-Gal staining, and mRNA expression of senescence markers in isolated cholangiocytes; however, *Kit<sup>W-sh</sup>* WD mice had decreased biliary senescence compared to WT WD mice (Figure 4C-E). MCs promote DR and mediate biliary senescence during NAFLD, which is also supported by our previous work(6).

#### **WD-Induced Inflammation, Hepatic Fibrosis and Hepatic Stellate Cell (HSC) Number are Reduced in MC-Deficient Mice**

Inflammation is key for NAFLD-NASH transition, and we found increased KC presence in WT WD mice compared to WT CD mice; however, *Kit<sup>W-sh</sup>* WD mice had decreased KC presence compared to WT WD mice (Figure 5A). Similar findings were shown for CCL3, CCL4, and CCL5 expression (Figure 5B) and IL-6 immunostaining (Figure 5C).

MC activation promotes liver fibrosis during cholestasis(10, 11), and WT WD mice had increased collagen deposition, Col1a1 expression and hydroxyproline content compared to WT CD mice; however, these findings were reduced in *Kit<sup>W-sh</sup>* WD mice compared to WT WD mice (Figure 5D, E). Similarly, HSC presence increased in WT WD mice compared to WT CD mice, as shown by desmin staining, but were markedly reduced in *Kit<sup>W-sh</sup>* WD mice compared to WT WD mice (Figure 5F).

#### **WD-Induced Vascular Endothelial Growth Factor (VEGF)-A Expression and Angiogenesis are Decreased in MC-Deficient Mice**

Previous work has shown that MC activation promotes angiogenesis and VEGF-A levels during cholestasis(9, 21). We found that hepatic VEGF-A expression increased in total liver and isolated cholangiocytes in WT WD mice compared to WT CD mice; however, VEGF-A gene expression (Supplemental Figure 3A) and immunoreactivity (Supplemental Figure 3B) decreased in *Kit<sup>W-sh</sup>* WD mice compared to WT WD mice. Additionally, NAFLD and NASH patients had increased

expression of VEGF-A (brown), along with increased MC presence (red), compared to controls (Supplemental Figure 3C).

WT WD mice had increased angiogenesis compared to WT CD mice, as demonstrated by vWF staining; however, *Kit<sup>W-sh</sup>* WD mice had reduced angiogenesis compared to WT WD mice (Supplemental Figure 3D). Importantly, vWF expression increased in NAFLD and NASH patients compared to controls (Supplemental Figure 3E), demonstrating that angiogenesis contributes to NAFLD/NASH.

#### ***Loss of MCs Reverses miR-144-3p Targeting of ALDH1A3 and Subsequent Lipid Peroxidation***

We found that MC loss primarily reduces zone 1 microvesicular steatosis (Figure 3A). The presence of microvesicular steatosis indicates a worsening phenotype, and is generally associated with impaired  $\beta$ -oxidation, oxidative stress and impaired toxin clearance(5). Suppression of ALDH1A3 has been noted in NAFLD patients(16); therefore, we postulated that MCs mediate microvesicular steatosis via ALDH1A3 dysregulation. We found that, in WT WD mice, there is increased MC presence (white arrows) corresponding with reduced ALDH1A3 expression when compared to WT CD mice; however, ALDH1A3 expression is restored in *Kit<sup>W-sh</sup>* WD mice compared to WT WD mice, shown by immunostaining and western blotting in isolated hepatocytes (Figure 6A). In human NASH samples there is reduced ALDH1A3 expression compared to controls, determined by immunostaining and western blotting in total liver (Figure 6B). No changes in the mRNA expression of ALDH1A3 were found in our mouse models or human samples (Supplemental Figure 4A, B) indicating post-transcriptional regulation.

Since we hypothesize that post-transcriptional modifications mediate ALDH1A3 suppression, we used TargetScan software to screen for various miRNA targets, and found that miR-144-3p was a highly conserved target for both mouse and human ALDH1A3 sequence (Figure 6C). miR-144-3p targeting of ALDH1A3 was verified by Ingenuity Pathway Analysis (IPA, Figure 6C). We found that miR-144-3p expression significantly increased in total liver and isolated hepatocytes from WT WD mice compared to WT CD mice; however, miR-144-3p expression decreased in *Kit<sup>W-sh</sup>* WD mice compared to WT WD mice (Figure 6D). In human samples, miR-144-3p levels were significantly increased in total liver from NASH patients compared to controls (Figure 6E). Lastly, by luciferase assay we determined that miR-144-3p targets and decreases the expression of Aldh1a3, but no targeting occurred in the mutated form of Aldh1a3 (Figure 6F).

ALDH1A3 downregulation is associated with lipid peroxidation(22), which can be a driver of microvesicular steatosis(23), and we found that hepatic MDA levels significantly increased in WT WD mice compared to WT CD mice, but significantly decreased in *Kit<sup>W-sh</sup>* WD mice compared to WT WD mice (Supplemental Figure 4C).

### **MC Injection Promotes Liver Damage and Microvesicular Steatosis During WD Feeding**

To demonstrate that MCs mediate WD-induced changes, we reintroduced MCs during the last 2 wks of feeding (Supplemental Figure 5A). Macroscopic liver images and LW/BW ratios are provided (Supplemental Figure 5B, C), and injected MCs (red) are found surrounding bile ducts (Supplemental Figure 5D).

H&E staining demonstrated that WT WD+MC mice presented with 30-90% steatosis, predominantly microvesicular steatosis, ranging from zone 1-2. Interestingly, there was more microvesicular, and less macrovesicular, steatosis in WT WD+MC mice compared to WD alone (Figure 7A), indicating a switch in steatotic phenotype. WT WD+MC mice had rare foci of inflammation and increased duct profiles in portal areas (not seen in WD alone) and were diagnosed with mild steatohepatitis (Figure 7A). MC injection into *Kit<sup>W-sh</sup>* WD mice (that presented with macrovesicular steatosis in zone 1 and microvesicular steatosis in zone 2 in mice without MC injection) now demonstrate microvesicular steatosis in zones 1 and 2 (Figure 7A). *Kit<sup>W-sh</sup>* WD+MC mice had mild DR and few foci of lobular inflammation, which was not present in WD alone, and were diagnosed with mild steatohepatitis (Figure 7A). MC injection promotes microvesicular steatosis development, particularly in zone 1 hepatocytes, which may be due to MC honing to portal areas.

MC injection into WT WD and *Kit<sup>W-sh</sup>* WD mice increased ALT levels compared to WD alone (Figure 7B). We have previously found that MC injection into normal *Kit<sup>W-sh</sup>* mice does not increase serum AST and ALT(9); therefore, MCs may exacerbate damage when an insult has already occurred.

Unexpectedly, lipid deposition was reduced in WT WD+MC mice compared to WT WD alone, which may indicate a worsening phenotype considering a loss of steatosis quantity in lieu of inflammation and fibrosis can be seen in NAFLD to NASH transition(5); however, MC injections increased lipid deposition in *Kit<sup>W-sh</sup>* WD mice compared to WD alone (Figure 7C). The increased lipid droplet area may be occurring in *Kit<sup>W-sh</sup>* WD mice, but not WT WD mice, since they previously did not have the same degree of WD-induced macrovesicular steatosis (Figure 3A, C). Therefore, H&E staining demonstrates a switch from primarily macrovesicular to microvesicular steatosis, which may

explain less lipid deposition in WT WD+MC mice. Similarly, hepatic TG levels were unchanged in WT WD+MC mice, but were significantly increased in *Kit<sup>W-sh</sup>* WD+MC mice compared to WD alone (Figure 7C).

#### ***MC Injection Promotes WD-Induced Biliary and Liver Damage, and miR-144-3p/ALDH1A3 Axis***

DR (Supplemental Figure 6A), biliary senescence (Supplemental Figure 6B) and inflammation (Supplemental Figure 6C) increased in both WT WD and *Kit<sup>W-sh</sup>* WD mice following MC injections compared to WD alone. Similarly, MC injection increased liver fibrosis and HSC presence in WT WD and *Kit<sup>W-sh</sup>* WD mice compared to WD alone (Supplemental Figure 7A, B). There was a larger degree of liver fibrosis in the WT WD mice injected with MCs than the *Kit<sup>W-sh</sup>* WD mice, which may be due to pre-existing liver damage.

MC injection into WT and *Kit<sup>W-sh</sup>* WD mice increased VEGF-A expression (Supplemental Figure 8A), and angiogenesis (Supplemental Figure 8B) compared to WD alone. Hepatic miR-144-3p expression increased, while ALDH1A3 expression decreased, and MDA levels increased in WT WD and *Kit<sup>W-sh</sup>* WD mice following MC injections (Supplemental Figure 8C-E). These findings confirm that MCs promote WD-induced biliary and liver damage, and may correspond with worsening phenotypes.

#### ***In Vitro, FFAs Promote Biliary Senescence, and Injured Cholangiocytes, but Not Hepatocytes, Drive MC Migration***

FFAs increase senescence and angiogenesis markers in cultured cholangiocytes compared to BS (Supplemental Figure 9A). Pooled cultured cholangiocytes, but not hepatocytes, pre-treated with FFAs increased MC migration compared to basal (BS) (Supplemental Figure 9B), which corresponds with our hypothesis that cholangiocyte-derived IGF-1 promotes MC migration. Furthermore, these *in vitro* findings confirm that MCs are drawn to injured cholangiocytes, but not hepatocytes, explaining why MCs are found near portal triads.

#### ***In Vitro, MC-Derived Histamine Promotes Biliary Senescence, Hepatocyte Steatosis, and Activation of KCs and HSCs***

*In vitro*, we treated MCs with compound 48/80 (to induce MC release of histamine), and found that histamine release significantly increased compared to MC BS (Supplemental Figure 10A). *In vitro*, Pool+MC treatments increased SA-β-Gal activity compared to BS treatment, and Pool+MC-

48/80 treatments (containing increased histamine levels) had a further increase in SA- $\beta$ -Gal activity compared to Pool+MC (Supplemental Figure 10B). Cultured mouse hepatocytes (i.e., mHep) were treated with FFAs, along with MC or MC-48/80 supernatants, to evaluate lipogenesis. Following FFA treatments, mHeps had increased lipid droplet area, which is further enhanced when FFA treatment is combined with MC supernatants (Supplemental Figure 10C). Interestingly, mHeps treated with FFAs and MC-48/80 supernatants have further increased lipid droplet deposition compared with FFA+MC treatments (Supplemental Figure 10C), highlighting the potential role for MC-derived histamine in the promotion of hepatocyte lipogenesis. Lastly, cultured mouse KCs (mKC) and mouse HSCs (mHSC) were treated with supernatants from MC or MC-48/80. mKC+MC had increased TNF- $\alpha$  immunoreactivity compared to BS, that was further increased in mKC+MC-48/80 treatments (Supplemental Figure 10D). Similarly, mHSC+MC showed increased  $\alpha$ -SMA immunoreactivity compared to BS, that was further enhanced in mHSC+MC-48/80 treatments (Supplemental Figure 10E).

## Discussion

MCs contribute to microvesicular steatosis, DR, biliary senescence, inflammation, angiogenesis, and hepatic fibrosis during NAFLD/NASH. MC deficiency reduces WD-induced injuries, and MC injections into WT and MC-deficient mice exacerbates damage. We propose that MCs drive worsening phenotypes, including microvesicular steatosis development, via miR-144-3p/ALDH1A3 signaling. Additionally, we found that following WD, biliary IGF-1 expression/secretion enhances and may induce MC infiltration near injured bile ducts. Our overall working model is presented in Figure 8.

DR (i) correlates with fibrosis staging in NAFLD patients(7), (ii) promotes oxidative stress in pediatric NAFLD patients and (iii) correlates with liver fibrosis in NASH patients(24). In our model, loss of MCs reduced WD-induced DR, which is promoted following MC injection. To support this finding, mice lacking histamine signaling have reduced DR following WD feeding; however, the impact of MCs or MC-derived histamine was not evaluated in this manuscript(6). In other reports, MC presence increases in patients and murine models of PSC, and inhibition of MC activation/histamine signaling or genetic loss of MCs reduces DR in these models(9, 21, 25). Furthermore, infiltrating MCs are found surrounding bile ducts(10, 11, 21), which mirrors the findings in this paper. Both parenchymal and periportal MC concentration increases in NASH, but total number of MCs and changes in MC infiltration are more prominent in the periportal region(26). We found that MCs were

adjacent to damaged ducts in our mouse model and human samples of NAFLD and NASH, and *in vitro* FFAs promote MC migration towards cholangiocytes, but not hepatocytes, via IGF-1. Others have found that MCs reside near portal areas in chronic liver diseases, and are predominantly found in cholestatic liver injuries(27). Additionally, it has been shown that IGF-1 promotes MC activation(20). This supports our hypothesis that injured cholangiocytes interact with MCs to promote migration during NAFLD/NASH. Hepatic IgE levels increased in WT WD mice, which may allude to the role of hepatic plasma cells or B cells in the promotion of MC infiltration and activation; however, cellular crosstalk between MCs and other immune cells requires further investigation.

Previous work found that mice lacking histamine signaling (that have fewer and morphologically altered MCs) have reduced WD-induced inflammation compared to WT WD mice(6). In our model, hepatic inflammation decreased in MC-deficient WD mice, which was reactivated following MC injection. Apolipoprotein E-deficient (*ApoE*<sup>-/-</sup>) mice that were crossed with *Kit*<sup>W-sh/W-sh</sup> (MC-deficient model) and subjected to HFD feeding had reduced IL-6 and IL-10 serum levels compared to *ApoE*<sup>-/-</sup> HFD mice(28), which is important considering patients with simple steatosis have increased IL-6 serum levels(29). Furthermore, we found *in vitro* that MC-derived histamine promotes KC activation. One study found that endogenous histamine synthesis in KCs protects from LPS-induced hepatitis via activation of the H2 histamine receptor (HR)(30), but others have found that H4HR activation promotes TNF- $\alpha$  synthesis in a rat model of LPS-induced inflammation(31). Our work has shown that histamine treatment increases KC number and liver inflammation in mice(32). Overall, MC and histamine impact on KCs is controversial, and may depend on HR expression.

There is a strong link between MC activation and liver fibrosis during cholestasis(9-11), and hepatic MC concentration correlates with fibrosis in NASH patients (26). Previous work found that loss of histamine signaling reduces liver fibrosis during WD feeding(6), and we found that liver fibrosis and HSC activation were reduced in MC-deficient WD mice, but MC injection exacerbates these parameters. Others have shown that inhibition of chymase (secreted by activated MCs) reduced liver fibrosis in hamsters fed a methionine- and choline-deficient diet(33), showing that MC inhibition reduces liver fibrosis. We have previously shown that HSCs express H1HR(10), and inhibition of MC activation blocks HSC activation and liver fibrosis in cholestatic models(9, 21). Furthermore, histamine treatment promotes liver fibrosis and HSC presence(32); however, the direct impact of histamine on HSCs is undefined and requires further work.

NAFLD patients have increased hepatic angiogenesis(34), and hepatic VEGF-A levels are increased in patients with NASH(29). Increased angiogenesis and VEGF-A expression are noted in

PSC patients(35), and, furthermore, MC number corresponds with hepatic VEGF levels and angiogenesis in mouse models of PSC and CCA(9, 10). In MCs isolated from BDL rats, there is increased VEGF-A expression and secretion(12) showing that hepatic MCs have a pro-angiogenic phenotype. We found that loss of MCs ameliorates VEGF-A levels and reduces angiogenesis in our NAFLD model. Similarly, previous work has found that loss of histamine synthesis reduces VEGF-A expression and subsequent angiogenesis in a mouse model of PSC(32).

One key finding of our research was that MCs predominantly modulate microvesicular steatosis development following WD feeding. Microvesicular steatosis is a separate entity from macrovesicular steatosis and correlates with higher grades of steatosis, NAS scores, fibrosis and diagnosis of NASH(5). Patients receiving allografts with >15% microvesicular steatosis have reduced graft survival and higher AST peaks immediately post-transplant(36). While increased microvesicular steatosis has been identified as a prognostic marker for NAFLD outcomes, the pathogenesis of this development is unknown. We found that MCs promote microvesicular steatosis development, suggesting that MC presence indicates a poor outcome, and others have found that MC density correlates with steatosis, inflammation and fibrosis in hepatitis C virus patients(37). It is unknown if MCs mediate macro and/or microvesicular steatosis; therefore, our findings are the first to suggest this mechanism. Interestingly, loss of MCs significantly reduced LW and LW/BW ratios, but had no effect on BW following WD. Previous work using heterozygous *Kit<sup>W-sh</sup>/Kit<sup>W-sh</sup>* (WBB6F1/J) mice found that these mice were protected from HFD-induced obesity(38). Our studies potentially diverge from these since we used a different model of MC deficiency (B6.Cg-*Kit<sup>W-sh</sup>*/HNihrJaeBsmGlliJ). Another group found that MC depletion using *Mcpt5-Cre R-DTA* mice is not associated with attenuated weight gain and hepatic steatosis following HFD feeding(39). Again, this is a different model of MC deficiency, and the authors fed for 21 weeks which is significantly longer than our 16 weeks of feeding. Lastly, the authors failed to evaluate DR, inflammation and hepatic fibrosis, which are key features of NAFLD/NASH.

Loss of MCs significantly reduces miR-144-3p levels, and to support this miR-144-3p expression is significantly increased in NASH patients versus non-NASH controls(40). Further, hepatic miR-144-3p levels are increased in obese insulin-resistant humans and mouse models(41). We propose that miR-144-3p targets ALDH1A3 to promote microvesicular steatosis, which is supported by bioinformatic analyses and luciferase assay. ALDH1A3 is key for clearing toxins and metabolizing aldehydes in cells and can modulate lipid peroxidation(22). Interestingly, others have found that NASH patients have decreased hepatic ALDH1A3 levels(16), which we noted in our

mouse model and human NASH samples. Butyrate, a short chain fatty acid, increases ALDH1A3 expression in intestinal epithelial cells(42), but no other studies have identified ALDH1A3 in steatosis development.

Loss of ALDH1A3 promotes lipid peroxidation(22), and it has been previously reported that PPAR- $\gamma$  suppresses ALDH1A3 expression in lung cancer, which exerts anti-proliferative effects via increased lipid peroxidation(22). We found that WD feeding induced lipid peroxidation, which was further enhanced with MC injections; therefore, we hypothesize that suppressed ALDH1A3 promotes lipid peroxidation during NASH. To our knowledge, there are no other studies that evaluate the role of ALDH1A3 in the promotion of lipid peroxidation and microvesicular steatosis; however, this hypothesis is still relevant considering that lipid peroxidation is key for steatohepatitis development in WD fed mice (23, 43), and humans with NAFLD have increased lipid peroxidation(13). Similarly, in mouse models of microvesicular steatosis there is enhanced lipid peroxidation(19) and it has been reported that MC activation promotes lipid peroxidation in neonatal rat colon(44).

In conclusion MCs promote WD-induced steatosis, DR, inflammation, liver fibrosis and angiogenesis. MC number increases in both NAFLD and NASH patients, but more prominently in NASH, where microvesicular steatosis is noted; therefore, we suggest that MCs promote NAFLD progression to NASH with worsening phenotypes (Figure 8). Additionally, worsening changes may be mediated by (i) miR-144-3p targeting of ALDH1A3 (promoting microvesicular steatosis) or (ii) MC-derived histamine driving biliary senescence, hepatocyte lipogenesis, KC activation and HSC fibrogenesis. Cromolyn sodium (MC stabilizer), and over-the-counter HR antagonists (i.e., mepyramine) reduce DR and liver fibrosis in cholestatic models(10, 11, 21); therefore, future work is necessary to understand if these therapeutics will benefit NAFLD or NASH patients. We propose that MC presence indicates worsening phenotypes in NAFLD/NASH, and blocking MC migration or activation may prove therapeutic for this subset of patients.

## References:

1. Popescu M, Popescu IA, Stanciu M, Cazacu SM, Ianosi NG, Comanescu MV, Singer CE, et al. Non-alcoholic fatty liver disease - clinical and histopathological aspects. Rom J Morphol Embryol 2016;57:1295-1302.
2. Ratziu V, Bonyhay L, Di Martino V, Charlotte F, Cavallaro L, Sayegh-Tainturier MH, Giral P, et al. Survival, liver failure, and hepatocellular carcinoma in obesity-related cryptogenic cirrhosis. Hepatology 2002;35:1485-1493.

3. Williams CD, Stengel J, Asike MI, Torres DM, Shaw J, Contreras M, Landt CL, et al. Prevalence of nonalcoholic fatty liver disease and nonalcoholic steatohepatitis among a largely middle-aged population utilizing ultrasound and liver biopsy: a prospective study. *Gastroenterology* 2011;140:124-131.
4. Fromenty B, Pessayre D. Inhibition of mitochondrial beta-oxidation as a mechanism of hepatotoxicity. *Pharmacol Ther* 1995;67:101-154.
5. Tandra S, Yeh MM, Brunt EM, Vuppalanchi R, Cummings OW, Unalp-Arida A, Wilson LA, et al. Presence and significance of microvesicular steatosis in nonalcoholic fatty liver disease. *J Hepatol* 2011;55:654-659.
6. Kennedy L, Hargrove L, Demieville J, Bailey JM, Dar W, Polireddy K, Chen Q, et al. Knockout of L-Histidine Decarboxylase Prevents Cholangiocyte Damage and Hepatic Fibrosis in Mice Subjected to High-Fat Diet Feeding via Disrupted Histamine/Leptin Signaling. *Am J Pathol* 2018;188:600-615.
7. Richardson MM, Jonsson JR, Powell EE, Brunt EM, Neuschwander-Tetri BA, Bhathal PS, Dixon JB, et al. Progressive fibrosis in nonalcoholic steatohepatitis: association with altered regeneration and a ductular reaction. *Gastroenterology* 2007;133:80-90.
8. Beaven MA. Our perception of the mast cell from Paul Ehrlich to now. *Eur J Immunol* 2009;39:11-25.
9. Hargrove L, Kennedy L, Demieville J, Jones H, Meng F, DeMorrow S, Karstens W, et al. Bile duct ligation-induced biliary hyperplasia, hepatic injury, and fibrosis are reduced in mast cell-deficient Kit(W-sh) mice. *Hepatology* 2017;65:1991-2004.
10. Kennedy L, Hargrove L, Demieville J, Karstens W, Jones H, DeMorrow S, Meng F, et al. Blocking H1/H2 histamine receptors inhibits damage/fibrosis in Mdr2(-/-) mice and human cholangiocarcinoma tumorigenesis. *Hepatology* 2018;68:1042-1056.
11. Kennedy LL, Hargrove LA, Graf AB, Francis TC, Hodges KM, Nguyen QP, Ueno Y, et al. Inhibition of mast cell-derived histamine secretion by cromolyn sodium treatment decreases biliary hyperplasia in cholestatic rodents. *Lab Invest* 2014;94:1406-1418.
12. Hargrove L, Graf-Eaton A, Kennedy L, Demieville J, Owens J, Hodges K, Ladd B, et al. Isolation and characterization of hepatic mast cells from cholestatic rats. *Lab Invest* 2016;96:1198-1210.

13. Konishi M, Iwasa M, Araki J, Kobayashi Y, Katsuki A, Sumida Y, Nakagawa N, et al. Increased lipid peroxidation in patients with non-alcoholic fatty liver disease and chronic hepatitis C as measured by the plasma level of 8-isoprostanate. *J Gastroenterol Hepatol* 2006;21:1821-1825.
14. Hsu LC, Chang WC, Hiraoka L, Hsieh CL. Molecular cloning, genomic organization, and chromosomal localization of an additional human aldehyde dehydrogenase gene, ALDH6. *Genomics* 1994;24:333-341.
15. Yin H, Xu L, Porter NA. Free radical lipid peroxidation: mechanisms and analysis. *Chem Rev* 2011;111:5944-5972.
16. Pettinelli P, Arendt BM, Teterina A, McGilvray I, Comelli EM, Fung SK, Fischer SE, et al. Altered hepatic genes related to retinol metabolism and plasma retinol in patients with non-alcoholic fatty liver disease. *PLoS One* 2018;13:e0205747.
17. MacDonald GA, Bridle KR, Ward PJ, Walker NI, Houglum K, George DK, Smith JL, et al. Lipid peroxidation in hepatic steatosis in humans is associated with hepatic fibrosis and occurs predominately in acinar zone 3. *J Gastroenterol Hepatol* 2001;16:599-606.
18. Fromenty B, Berson A, Pessayre D. Microvesicular steatosis and steatohepatitis: role of mitochondrial dysfunction and lipid peroxidation. *J Hepatol* 1997;26 Suppl 1:13-22.
19. Natarajan SK, Eapen CE, Pullimood AB, Balasubramanian KA. Oxidative stress in experimental liver microvesicular steatosis: role of mitochondria and peroxisomes. *J Gastroenterol Hepatol* 2006;21:1240-1249.
20. Lessmann E, Grochow G, Weingarten L, Giesemann T, Aktories K, Leitges M, Krystal G, et al. Insulin and insulin-like growth factor-1 promote mast cell survival via activation of the phosphatidylinositol-3-kinase pathway. *Exp Hematol* 2006;34:1532-1541.
21. Jones H, Hargrove L, Kennedy L, Meng F, Graf-Eaton A, Owens J, Alpini G, et al. Inhibition of mast cell-secreted histamine decreases biliary proliferation and fibrosis in primary sclerosing cholangitis Mdr2(-/-) mice. *Hepatology* 2016;64:1202-1216.
22. Hua TNM, Namkung J, Phan ANH, Vo VTA, Kim MK, Jeong Y, Choi JW. PPARgamma-mediated ALDH1A3 suppression exerts anti-proliferative effects in lung cancer by inducing lipid peroxidation. *J Recept Signal Transduct Res* 2018;38:191-197.
23. Morita M, Ishida N, Uchiyama K, Yamaguchi K, Itoh Y, Shichiri M, Yoshida Y, et al. Fatty liver induced by free radicals and lipid peroxidation. *Free Radic Res* 2012;46:758-765.

24. Nobili V, Carpino G, Alisi A, Franchitto A, Alpini G, De Vito R, Onori P, et al. Hepatic progenitor cells activation, fibrosis, and adipokines production in pediatric nonalcoholic fatty liver disease. *Hepatology* 2012;56:2142-2153.
25. Johnson C, Huynh V, Hargrove L, Kennedy L, Graf-Eaton A, Owens J, Trzeciakowski JP, et al. Inhibition of Mast Cell-Derived Histamine Decreases Human Cholangiocarcinoma Growth and Differentiation via c-Kit/Stem Cell Factor-Dependent Signaling. *Am J Pathol* 2016;186:123-133.
26. Lombardo J, Broadwater D, Collins R, Cebe K, Brady R, Harrison S. Hepatic mast cell concentration directly correlates to stage of fibrosis in NASH. *Hum Pathol* 2019;86:129-135.
27. Yamashiro M, Kouda W, Kono N, Tsuneyama K, Matsui O, Nakanuma Y. Distribution of intrahepatic mast cells in various hepatobiliary disorders. An immunohistochemical study. *Virchows Arch* 1998;433:471-479.
28. Smith DD, Tan X, Raveendran VV, Tawfik O, Stechschulte DJ, Dileepan KN. Mast cell deficiency attenuates progression of atherosclerosis and hepatic steatosis in apolipoprotein E-null mice. *Am J Physiol Heart Circ Physiol* 2012;302:H2612-2621.
29. Coulon S, Francque S, Colle I, Verrijken A, Blomme B, Heindryckx F, De Munter S, et al. Evaluation of inflammatory and angiogenic factors in patients with non-alcoholic fatty liver disease. *Cytokine* 2012;59:442-449.
30. Yokoyama M, Yokoyama A, Mori S, Takahashi HK, Yoshino T, Watanabe T, Watanabe T, et al. Inducible histamine protects mice from *P. acnes*-primed and LPS-induced hepatitis through H2-receptor stimulation. *Gastroenterology* 2004;127:892-902.
31. Ahmad SF, Ansari MA, Zoheir KM, Bakheet SA, Korashy HM, Nadeem A, Ashour AE, et al. Regulation of TNF-alpha and NF-kappaB activation through the JAK/STAT signaling pathway downstream of histamine 4 receptor in a rat model of LPS-induced joint inflammation. *Immunobiology* 2015;220:889-898.
32. Kennedy L, Meadows V, Demieville J, Hargrove L, Virani S, Glaser S, Zhou T, et al. Biliary damage and liver fibrosis are ameliorated in a novel mouse model lacking l-histidine decarboxylase/histamine signaling. *Lab Invest* 2020;100:837-848.
33. Tashiro K, Takai S, Jin D, Yamamoto H, Komeda K, Hayashi M, Tanaka K, et al. Chymase inhibitor prevents the nonalcoholic steatohepatitis in hamsters fed a methionine- and choline-deficient diet. *Hepatol Res* 2010;40:514-523.

34. Ciupinska-Kajor M, Hartleb M, Kajor M, Kukla M, Wylezol M, Lange D, Liszka L. Hepatic angiogenesis and fibrosis are common features in morbidly obese patients. *Hepatol Int* 2013;7:233-240.
35. Wu N, Meng F, Zhou T, Han Y, Kennedy L, Venter J, Francis H, et al. Prolonged darkness reduces liver fibrosis in a mouse model of primary sclerosing cholangitis by miR-200b down-regulation. *FASEB J* 2017;31:4305-4324.
36. Ferri F, Lai Q, Molinaro A, Poli E, Parlati L, Lattanzi B, Mennini G, et al. Donor Small-Droplet Macrovesicular Steatosis Affects Liver Transplant Outcome in HCV-Negative Recipients. *Can J Gastroenterol Hepatol* 2019;2019:5862985.
37. Franceschini B, Russo C, Dioguardi N, Grizzi F. Increased liver mast cell recruitment in patients with chronic C virus-related hepatitis and histologically documented steatosis. *J Viral Hepat* 2007;14:549-555.
38. Liu J, Divoux A, Sun J, Zhang J, Clement K, Glickman JN, Sukhova GK, et al. Genetic deficiency and pharmacological stabilization of mast cells reduce diet-induced obesity and diabetes in mice. *Nat Med* 2009;15:940-945.
39. Chmelar J, Chatzigeorgiou A, Chung KJ, Prucnal M, Voehringer D, Roers A, Chavakis T. No Role for Mast Cells in Obesity-Related Metabolic Dysregulation. *Front Immunol* 2016;7:524.
40. Vega-Badillo J, Gutierrez-Vidal R, Hernandez-Perez HA, Villamil-Ramirez H, Leon-Mimila P, Sanchez-Munoz F, Moran-Ramos S, et al. Hepatic miR-33a/miR-144 and their target gene ABCA1 are associated with steatohepatitis in morbidly obese subjects. *Liver Int* 2016;36:1383-1391.
41. Azzimato V, Jager J, Chen P, Morgantini C, Levi L, Barreby E, Sulen A, et al. Liver macrophages inhibit the endogenous antioxidant response in obesity-associated insulin resistance. *Sci Transl Med* 2020;12.
42. Schilderink R, Verseijden C, Seppen J, Muncan V, van den Brink GR, Lambers TT, van Tol EA, et al. The SCFA butyrate stimulates the epithelial production of retinoic acid via inhibition of epithelial HDAC. *Am J Physiol Gastrointest Liver Physiol* 2016;310:G1138-1146.
43. Letteron P, Fromenty B, Terris B, Degott C, Pessayre D. Acute and chronic hepatic steatosis lead to in vivo lipid peroxidation in mice. *J Hepatol* 1996;24:200-208.
44. Brown JF, Chafee KA, Tepperman BL. Role of mast cells, neutrophils and nitric oxide in endotoxin-induced damage to the neonatal rat colon. *Br J Pharmacol* 1998;123:31-38.

#### Figure Legends:

**Figure 1:** Biliary IGF-1 secretion and expression. **(A)** Cytokine multiELISA showed increased release of IGF-1, IL-6, FGF-β, IFN-γ, EGF, Leptin, IL-17A, Resistin and IL-10 in WT WD mice compared to WT CD mice. **(B)** Fold change of the increased cytokines. **(C)** IgE levels in liver lysates increased in WT WD mice compared to WT CD mice. **(D)** IGF-1 secretion is increased in cholangiocyte supernatants and serum from WT WD mice compared to WT CD mice. **(E)** IGF-1 immunoreactivity is enhanced in WT WD mice compared to WT CD mice. **(F)** IGF-1 immunoreactivity is enhanced in human NASH compared to normal. n=3 reactions from n=10-15 mice for multiELISA, n=4 reaction from n=4 mice for IgE ELISA, n=4 reactions from n=8-10 mice for IGF-1 EIA. Data are mean±SEM. \*P<0.05 vs. WT CD mice. IGF-1 immunostaining shown at 20X and 60X.

**Figure 2:** MC presence and activation. WT WD mice had increased **(A)** mMCP-1 (MC marker, red arrows) expression; **(B)** chymase, tryptase and c-Kit mRNA expression and **(C)** serum histamine levels. **(D)** MCs (tryptase) and DR (CK-19) increased in NAFLD and NASH patients. **(E)** Chymase, tryptase and c-Kit mRNA expression increased in human NASH. n=4 reactions from n=10-15 mice for qPCR, n=2-4 reactions per samples from n=9 normal, n=9 NAFLD and n=17 NASH human samples for qPCR, n=4 reactions from n=10-15 mice for EIA. Data are mean±SEM. \*P<0.05 vs. WT CD mice or human normal. mMCP-1 immunostaining shown at 20X and 40X, tryptase/CK-19 co-immunostaining shown at 20X.

**Figure 3:** Liver steatosis and hepatocyte lipogenesis. **(A)** H&E showed increased steatosis, inflammation and DR in WT WD mice, which was reduced in *Kit<sup>W-sh</sup>* WD mice. **(B)** Serum ALT increased WT WD mice compared to WT CD mice, but decreased in *Kit<sup>W-sh</sup>* WD mice compared to WT WD mice. **(C)** By Oil Red O staining, % lipid droplet area increased in WT WD mice, which was reduced in *Kit<sup>W-sh</sup>* WD mice. Similar findings were noted for hepatic TG content. **(D)** Lipogenesis markers FASN, Acaca and PPAR-γ were increased in hepatocytes from WT WD mice compared to WT CD mice, but reduced in *Kit<sup>W-sh</sup>* WD mice compared to WT WD mice. β-oxidation markers Cpt1a, Cpt2 and PPAR-α mRNA expression decreased in hepatocytes from WT WD mice compared to WT CD mice, but increased in *Kit<sup>W-sh</sup>* WD mice compared to WT WD mice. n=4 reactions from n=8-15 mice for ALT, n=10 images from n=8-15 mice for Oil Red O, n=4 reactions from n=8-15 mice for TG EIA, n=4 reactions from n=8-15 mice for qPCR. Data are mean±SEM. \*P<0.05 vs. WT CD mice; #P<0.05 vs. WT WD mice. H&E shown at 10X, Oil Red O shown at 20X.

**Figure 4:** Ductular reaction and biliary senescence. **(A)** Immunostaining for CK-19 and **(B)** Ki67 indicated increased DR and biliary proliferation (red arrows) in WT WD mice compared to WT CD mice, which decreased in *Kit<sup>W-sh</sup>* WD mice compared to WT CD mice. Immunofluorescence for **(C)** p16 and **(D)** SA-b-Gal (both co-stained with CK-19) showed enhanced biliary senescence in WT WD mice compared to WT CD mice, that decreased in *Kit<sup>W-sh</sup>* WD mice compared to WT CD mice. **(E)** Expression of senescence markers increased in isolated cholangiocytes from WT WD mice compared to WT CD mice, but reduced in *Kit<sup>W-sh</sup>* WD mice compared to WT WD mice. n=10 images from n=8 mice for CK-19 and Ki67, n=4 reactions from n=8-15 mice for qPCR. Data are mean±SEM. \*P<0.05 vs. WT CD mice; #P<0.05 vs. WT WD mice. CK-19 and Ki67 staining shown at 20X, p16/CK-19 staining shown at 160X, SA-b-Gal/CK-19 staining shown at 80X.

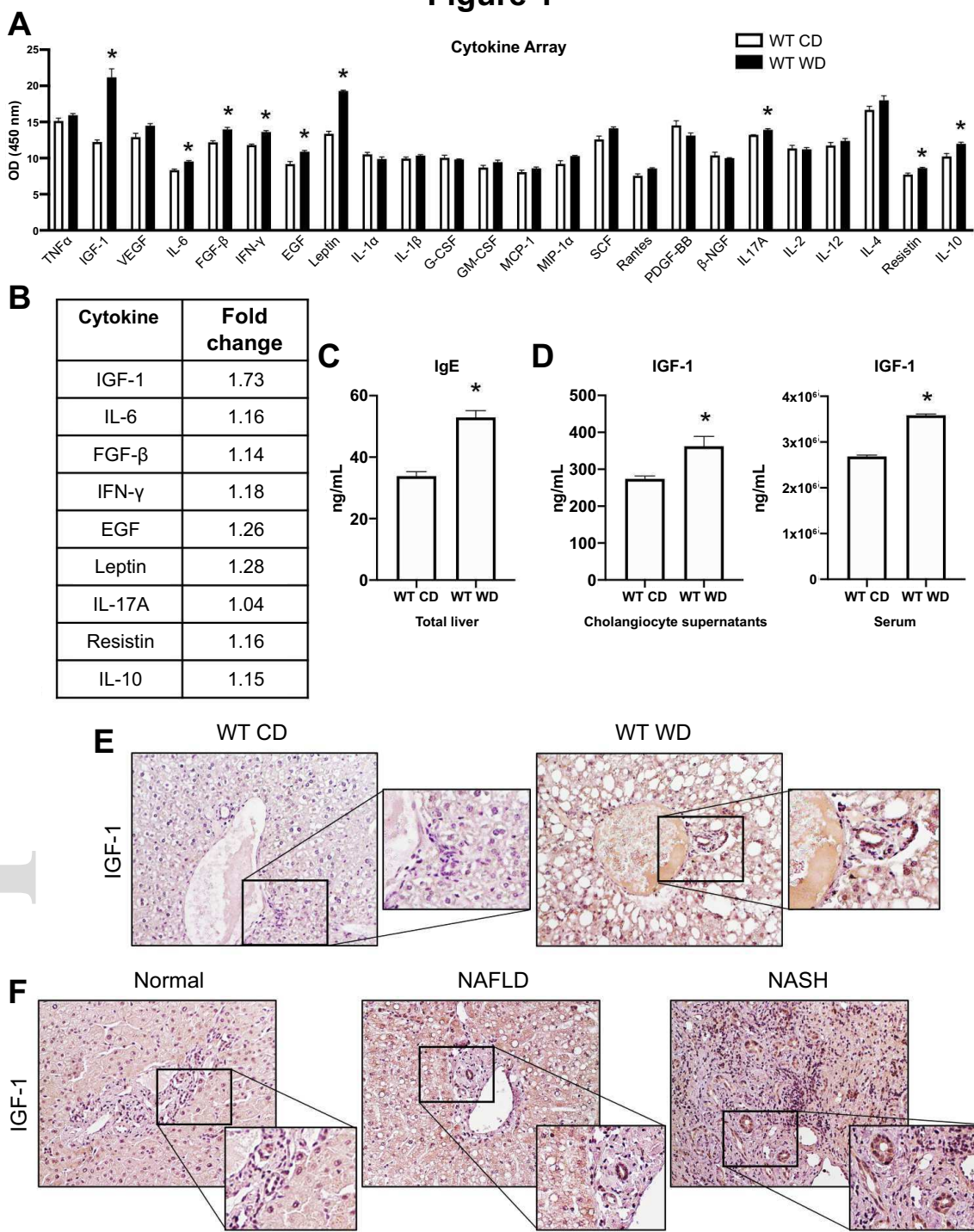
**Figure 5:** KC presence, liver inflammation and liver fibrosis. WT WD mice had increased: **(A)** KC presence; **(B)** CCL3, CCL4 and CCL5 mRNA expression and **(C)** IL-6 expression compared to WT CD mice, which decreased in *Kit<sup>W-sh</sup>* WD mice. WT WD mice had increased **(D)** collagen deposition (Sirius Red/Fast Green); **(E)** Col1a1 mRNA expression and hydroxyproline levels; and **(F)** desmin expression (HSC marker) compared with WT CD mice, but these parameters were decreased in *Kit<sup>W-sh</sup>* WD mice compared to WT WD mice. n=4 reactions from n=8-10 mice for qPCR, n=10 images from n=8-10 mice for staining, n=6 reactions from n=8-10 mice for hydroxyproline assay. Data are mean±SEM. \*P<0.05 vs. WT CD mice; #P<0.05 vs. WT WD mice. Immunostaining shown at 10X for F4/80 and 20X for IL-6, Sirius Red/Fast Green shown at 10X, desmin staining shown at 20X.

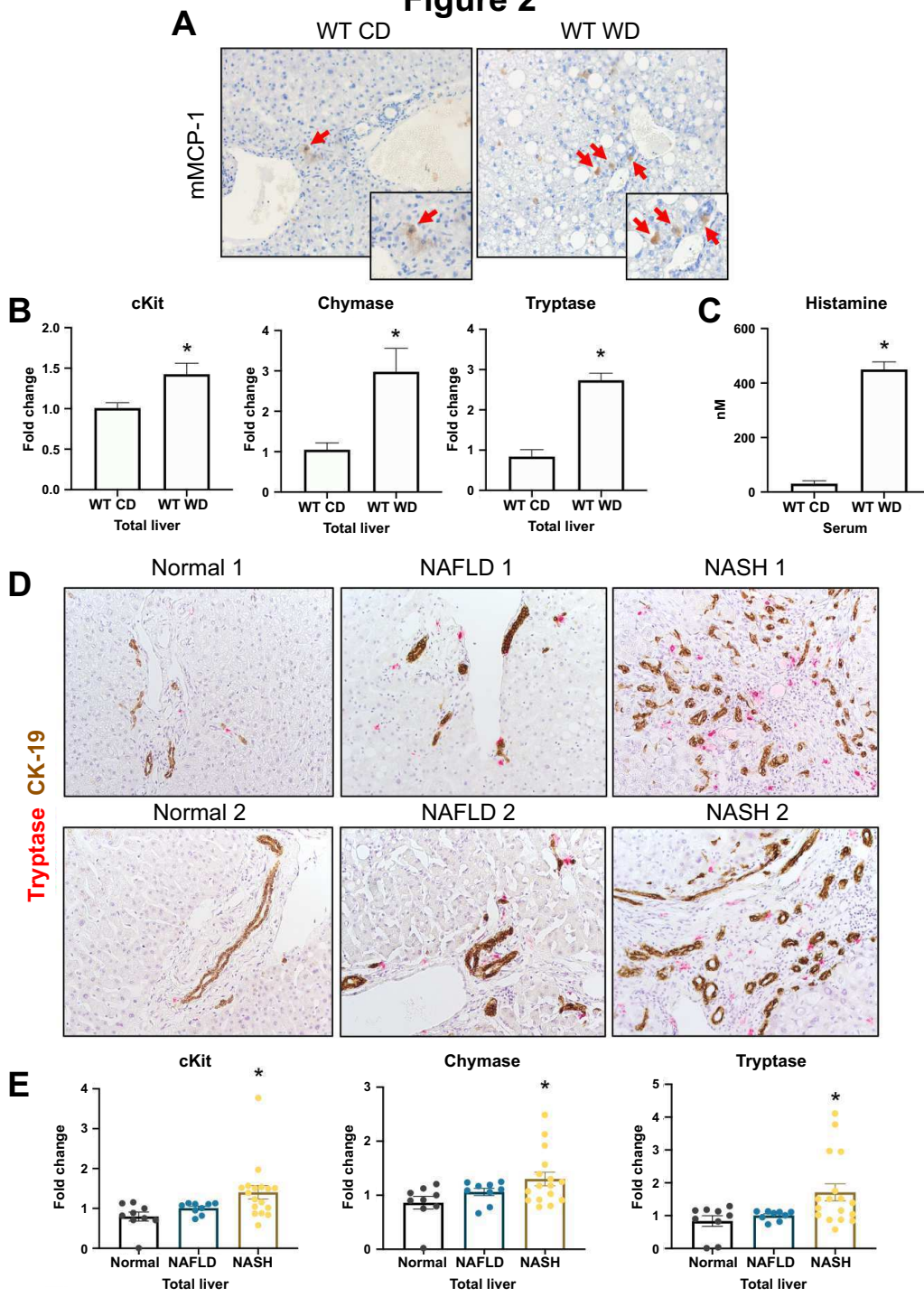
**Figure 6:** miR-144-3p/ALDH1A3 signaling mechanism. **(A)** ALDH1A3 expression is reduced in WT WD mice, concomitant with increased MC presence (white arrows) compared to WT CD mice, but this is reversed in *Kit<sup>W-sh</sup>* WD mice compared to WT CD mice, as indicated by immunostaining and western blotting. **(B)** ALDH1A3 expression is unchanged in human NAFLD compared to normal, but reduced in human NASH, as determined by immunostaining and western blotting. **(C)** TargetScan software identified miR-144-3p as a highly conserved miRNA targeting ALDH1A3, and miR-144-3p targeting of ALDH1A3 was confirmed by IPA. **(D)** miR-144-3p expression is increased in total liver and isolated hepatocytes from WT WD mice compared to WT CD mice, but decreased in *Kit<sup>W-sh</sup>* WD mice compared to WT WD mice. **(E)** Similarly, miR-144-3p expression is increased in human NASH compared to normal; there is no change between NAFLD and normal. **(F)** By luciferase assay, miR-144-3p significantly decreases Aldh1a3-WT expression, but this downregulation is ablated Aldh1a3-

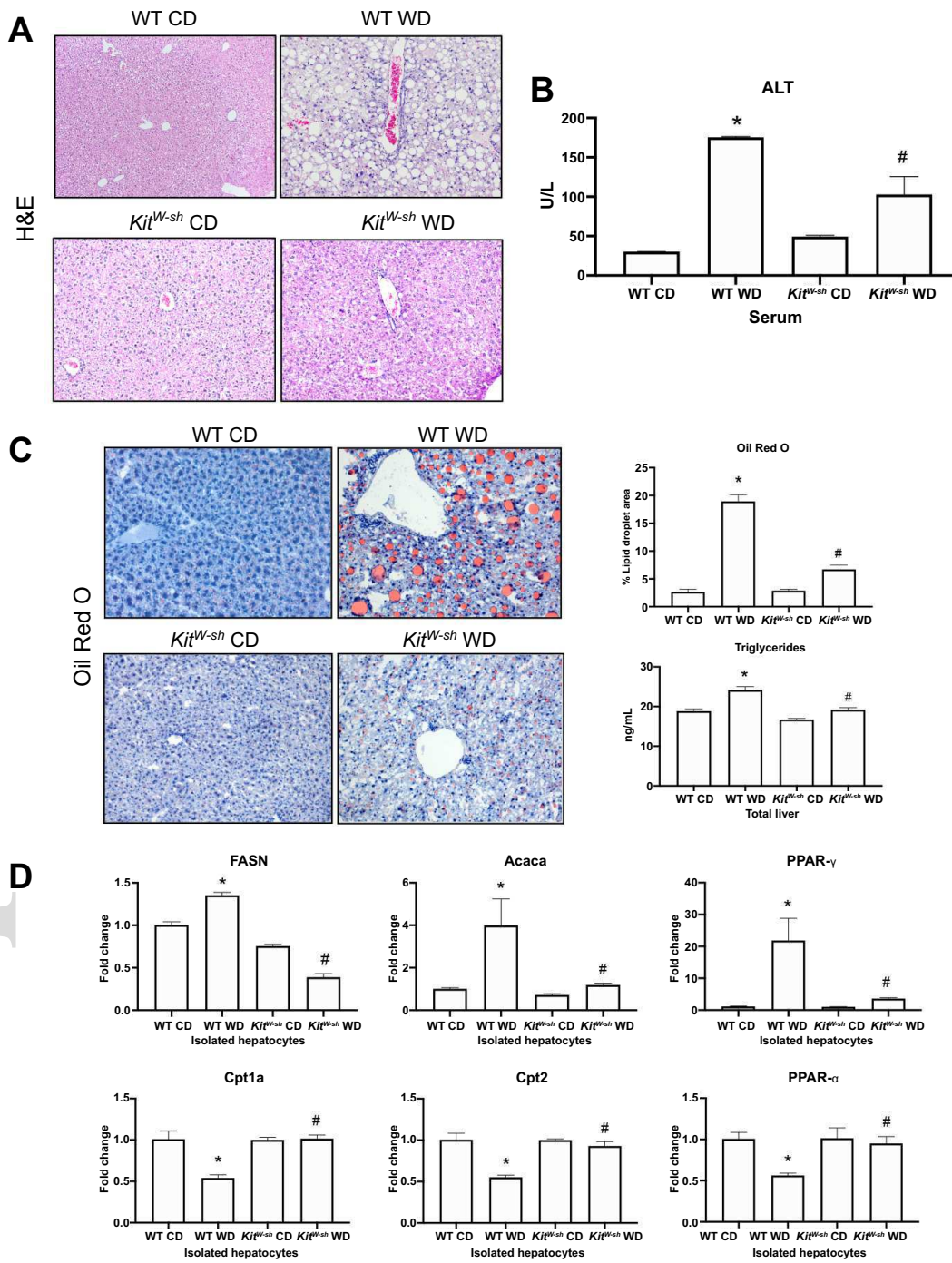
MUT form. n=6 bands from n=10-15 mice for western blotting, n=1 band per sample from n=4 normal, n=9 NAFLD and n=7 NASH total liver samples for western blotting, n=9-12 reactions for total liver and n=3 reactions for isolated hepatocytes from n=10-15 mice for qPCR, n=3 reactions per sample from n=4 normal, n=12 NAFLD and n=14 NASH for human total liver qPCR, n=5 reactions for luciferase assay. Data are mean $\pm$ SEM. \*P<0.05 vs. WT CD mice, miRNA NC or normal human patient; #P<0.05 vs. WT WD mice. Mouse staining shown at 80X, and human staining shown at 40X.

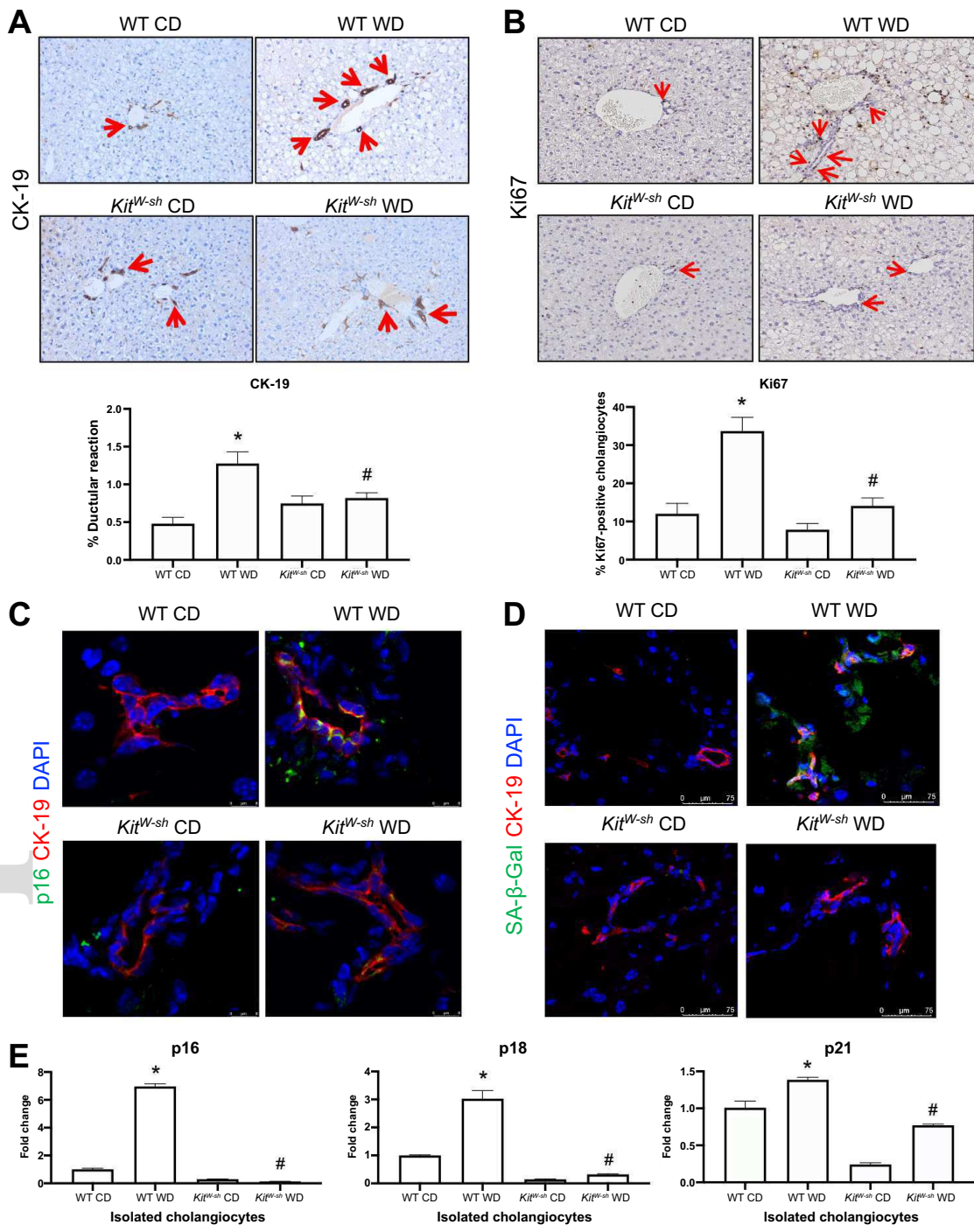
**Figure 7:** Changes in liver damage and steatosis following MC injections. **(A)** Microvesicular steatosis, inflammation and DR increased in WT WD+MC mice compared to WT WD mice. *Kit<sup>W-sh</sup>* WD+MC mice had increased microvesicular steatosis, inflammation and DR compared to *Kit<sup>W-sh</sup>* WD mice. **(B)** Serum levels of ALT are significantly increased in WT WD and *Kit<sup>W-sh</sup>* WD mice following MC injections compared to controls. **(C)** Oil Red O staining showed a reduction in lipid droplet area (indicative of microvesicular steatosis development) in WT WD+MC mice compared to WT WD mice; however, *Kit<sup>W-sh</sup>* WD+MC mice had an increase in lipid droplet area compared to *Kit<sup>W-sh</sup>* WD mice. Hepatic TGs are unchanged in WT WD+MC mice compared to WT WD mice, but increased in *Kit<sup>W-sh</sup>* WD+MC mice compared to *Kit<sup>W-sh</sup>* WD mice. n=5 reactions for serum chemistry from n=10-13 mice, n=10 images from n=10-13 mice for Oil Red O staining, n=4 reactions from n=10-13 mice for TG EIA. Data are mean $\pm$ SEM. \*P<0.05 vs. WT WD mice or *Kit<sup>W-sh</sup>* WD mice. H&E staining shown at 10X, Oil Red O staining shown at 20X.

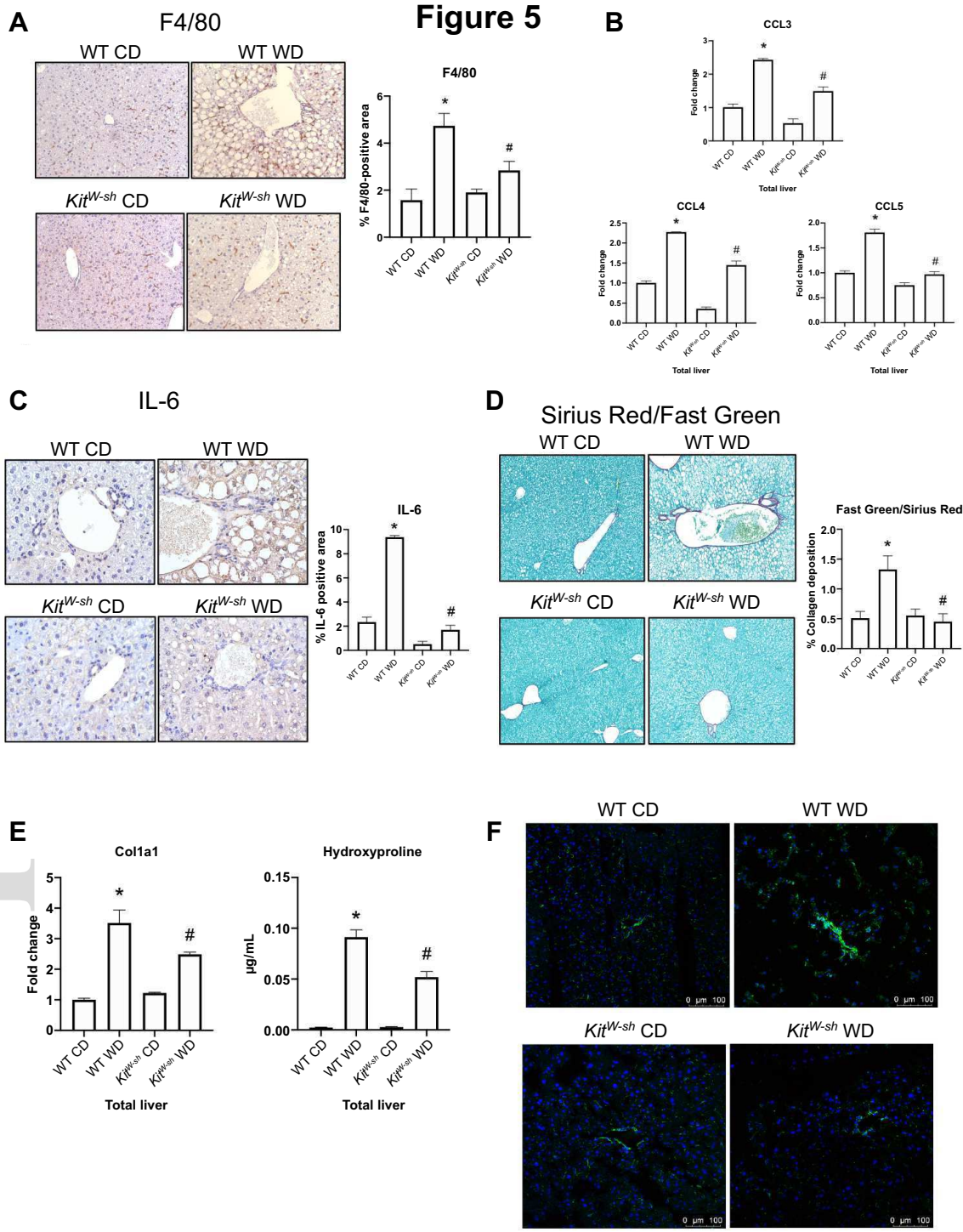
**Figure 8:** Working model. During NAFLD progression to NASH, bile ducts are injured and increase secretion of IGF-1, which promotes MC migration to the portal areas. Enhanced MC migration and activation increases miR-144-3p expression in hepatocytes, which inhibits and downregulates ALDH1A3 expression. Image made with BioRender.

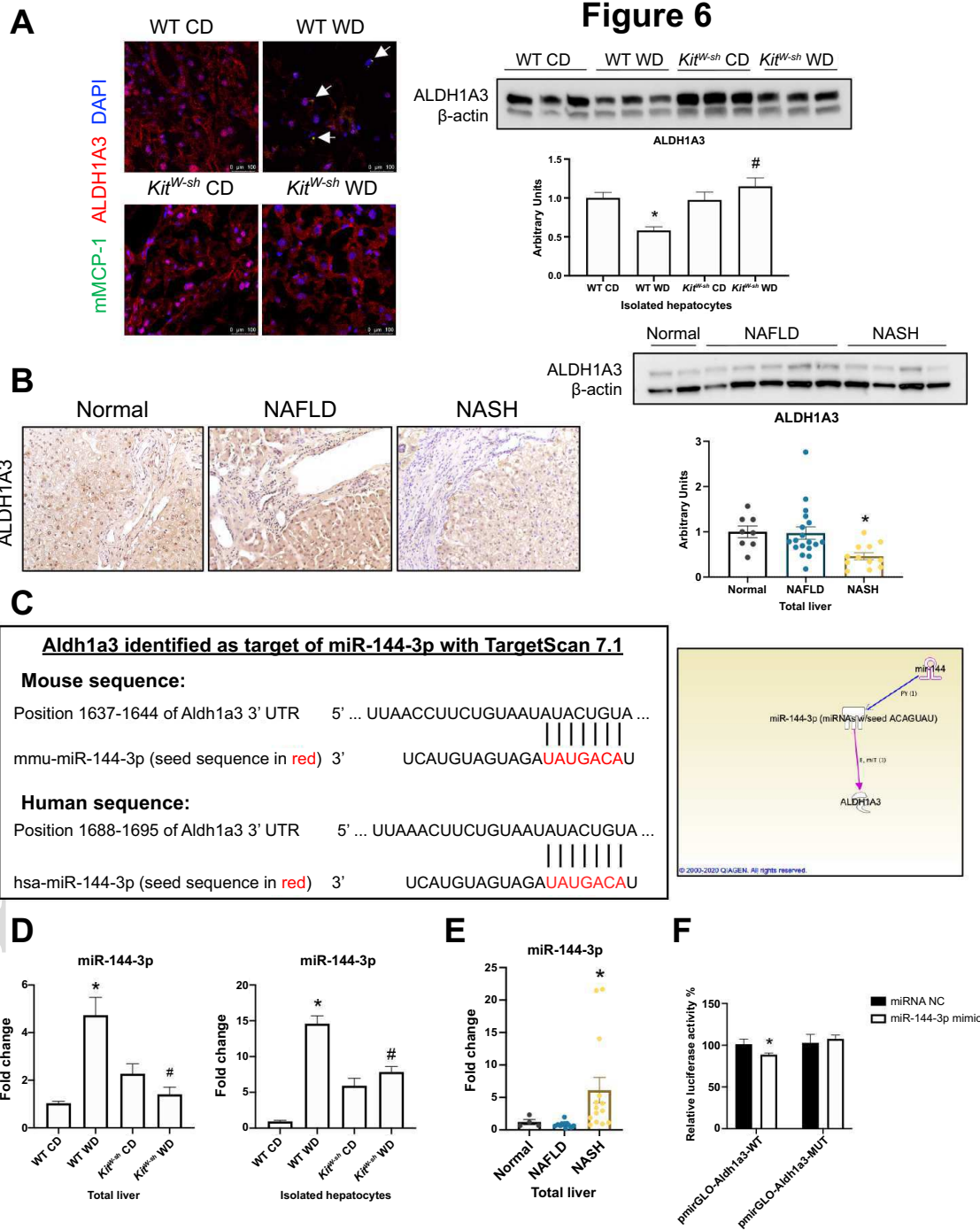
**Figure 1**

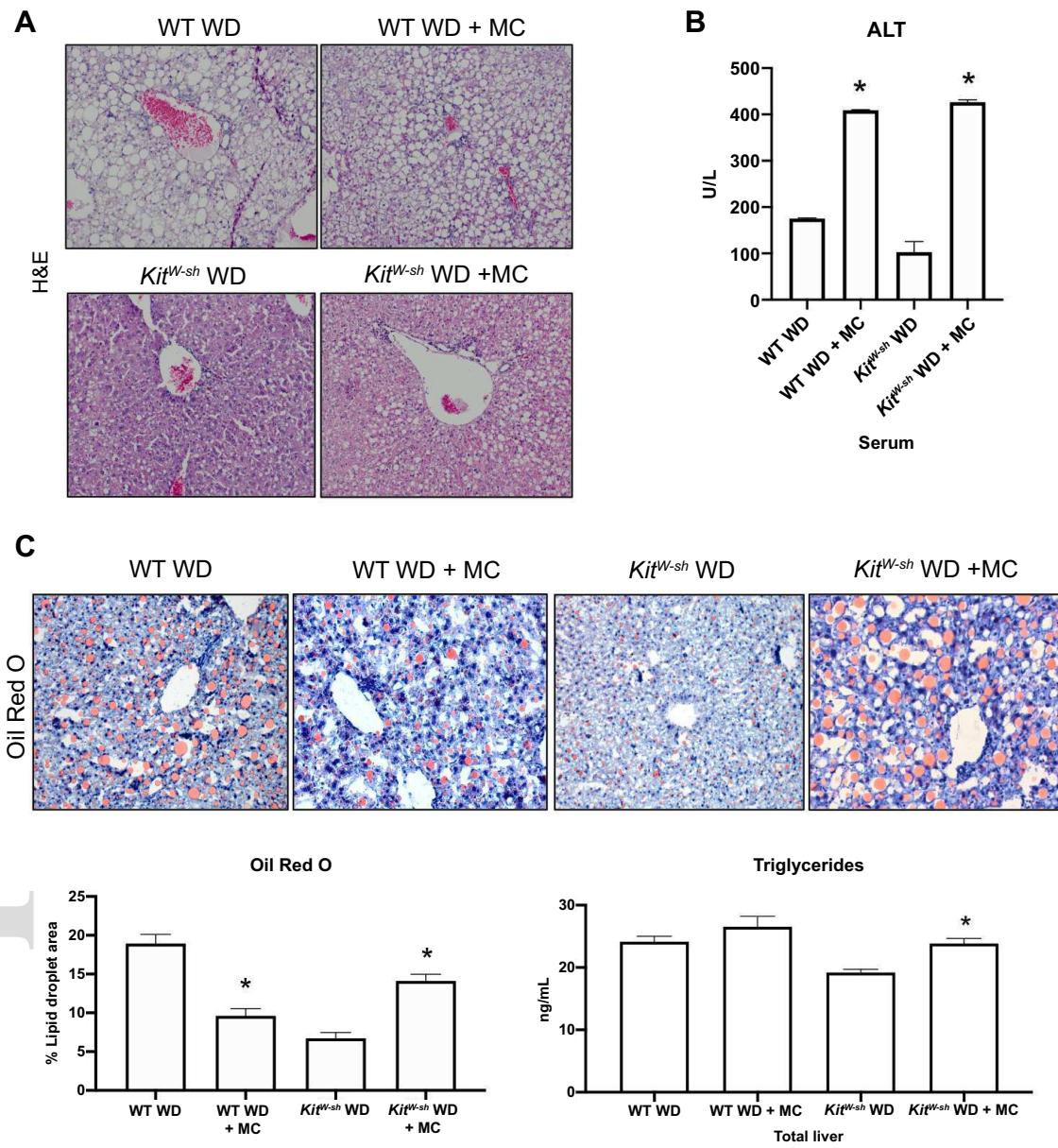
**Figure 2**

**Figure 3**

**Figure 4**

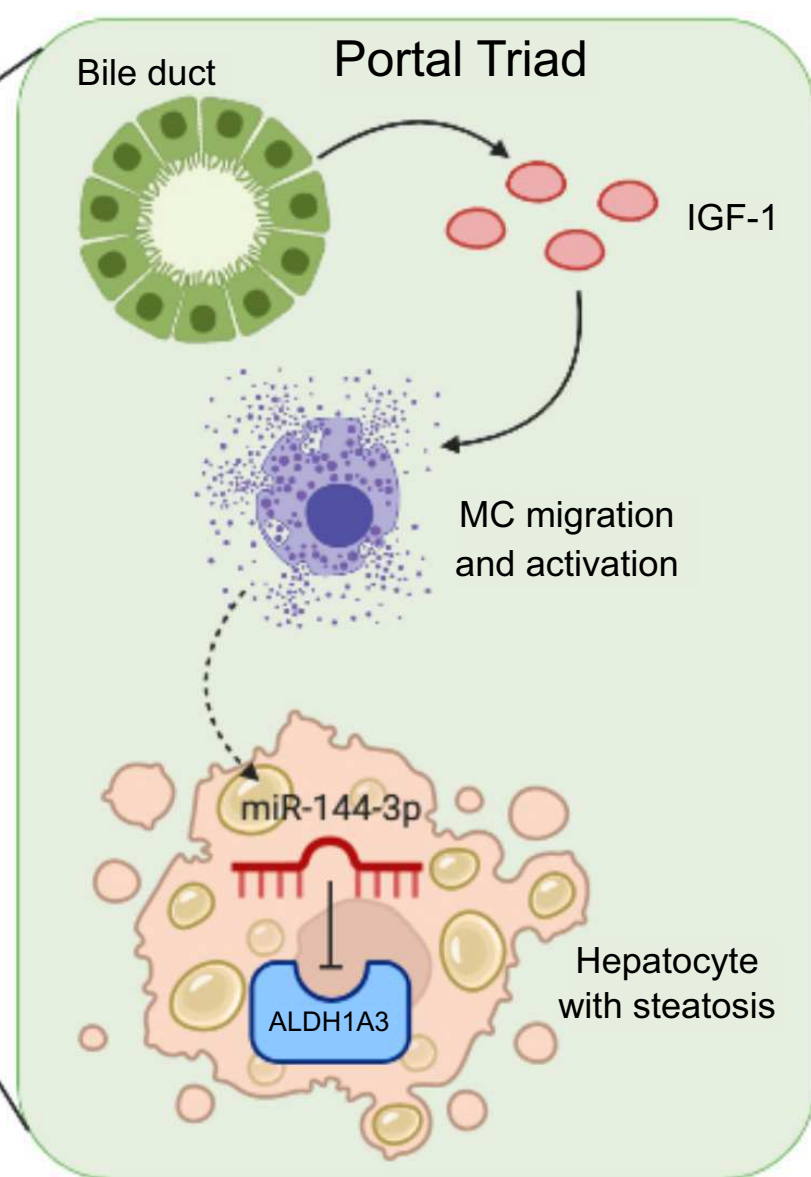
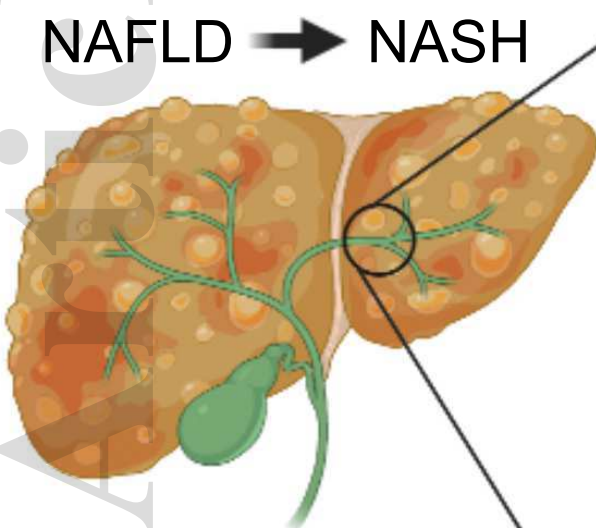
**Figure 5**

**Figure 6**

**Figure 7**

**Figure 8**

Accepted Article



hep\_31713\_f8.eps